Carbohydrate Polymers 83 (2011) 1804–1811

Contents lists available at ScienceDirect

Carbohydrate Polymers

journal homepage: www.elsevier.com/locate/carbpol

Individualization of cellulose nanofibers from wood using high-intensity ultrasonication combined with chemical pretreatments

Wenshuai Chen[a,b], Haipeng Yu[a,b,*], Yixing Liu[a,b], Peng Chen[b], Mingxin Zhang[b], Yunfei Hai[b]

[a] Key Laboratory of Bio-based Material Science and Technology of Ministry of Education, Northeast Forestry University, Harbin 150040, China
[b] Material Science and Engineering College, Northeast Forestry University, Harbin 150040, China

ARTICLE INFO

Article history:
Received 7 July 2010
Received in revised form 12 October 2010
Accepted 20 October 2010
Available online 27 October 2010

Keywords:
Cellulose nanofibers
Chemical treatment
Ultrasonic treatment
Microstructure
Wood

ABSTRACT

Cellulose nanofibers were individualized from poplar wood in two distinct stages. Initially, wood fibers were subjected to a chemical process to eliminate lignin and hemicellulose. The obtained chemical-purified cellulose fibers were then mechanically separated into nanofibers using high-intensity ultrasonication. The diameter distributions of the resulting nanofibers were dependent on the output power of the ultrasonic treatment. TEM and FE-SEM images showed that the diameter of the obtained nanofibers ranged from 5 to 20 nm when the output power of the conducted ultrasonication was greater than 1000 W. FTIR and XRD results indicated that hemicellulose and lignin were removed extensively in the cellulose nanofibers, with a crystallinity of approximately 69%. The TGA results showed that the degradation temperature of the nanofibers was dramatically increased to approximately 335 °C compared with 210 °C of the original wood fibers. The obtained nanofibers may be potentially applied in various fields, such as bio-nanocomposites, tissue engineering scaffolds, filtration media, packaging, and so on.

1. Introduction

Cellulose is one of the most important biopolymers. It is widely used because of its availability, biocompatibility, biological degradability, and sustainability. Cellulose fibers exhibit a unique structural hierarchy derived from their biological origin. They are composed of nanofiber assemblies with a diameter that range from 2 to 20 nm, and a length of more than a few micrometers. These nanometer-sized single fibers of cellulose, which are commonly referred to as nanocrystals, whiskers, nanowhiskers, microfibrillated cellulose, microfibril aggregates or nanofibers (reviewed in Azizi Samir, Alloin, & Dufresne, 2005; Eichhorn et al., 2010; Siró & Plackett, 2010), can be obtained from various sources such as wood fibers (Abe, Iwamoto, & Yano, 2007), cotton (de Morais Teixeira et al., 2010), potato tuber cells (Dufresne, Dupeyre, & Vignon, 2000), both cladodes and spines from *Opuntia ficus-indica* (Malainine et al., 2003), prickly pear fruits of *O. ficus-indica* (Habibi, Heux, Mahrouz, & Vignon, 2008), lemon and maize (Rondeau-Mouro et al., 2003), soybean (Wang & Sain, 2007), wheat straw and soy hulls (Alemdar & Sain, 2008), hemp fiber (Wang, Sain, & Oksman, 2007), coconut husk fibers (Rosa et al., 2010), branch-barks of mulberry (Li et al., 2009), pineapple leaf fibres (Cherian et al., 2010), banana rachis (Zuluaga et al., 2009), sisal (Morán, Alvarez, Cyras, & Vázquez, 2008), pea hull fibre (Chen, Liu, Chang, Cao, & Anderson, 2009) and sugar beet (Dinand, Chanzy, & Vignon, 1999; Dufresne, Cavaillé, & Vignon, 1997). The individualization of cellulose nanofibers from renewable sources has gained more attention in recent years because of their exceptional mechanical properties (high specific strength and modulus), large specific surface area, low coefficient of thermal expansion, high aspect ratio, environmental benefits, and low cost (Nishino, Matsuda, & Hirao, 2004; Orts et al., 2005). Suitable applications of cellulose nanofibers, such as reinforcement components in flexible display panels (Iwamoto, Nakagaito, & Yano, 2007; Yano et al., 2005) and oxygen-barrier layers (Fukuzumi, Saito, Iwata, Kumamoto, & Isogai, 2009; Syverud & Stenius, 2009), have been proposed as well.

Several processes have been used to extract highly purified nanofibers from cellulosic materials. These methods include mechanical treatments, e.g., cryocrushing (Chakraborty, Sain, & Kortschot, 2005, 2006), grinding (see Abe et al., 2007; Abe, Nakatsubo, & Yano, 2009; Abe & Yano, 2009, 2010; Nogi, Iwamoto, Nakagaito, & Yano, 2009 and references therein), and high-pressure homogenizing (see Herrick, Casebier, & Hamilton, 1983; Nakagaito & Yano, 2004, 2005, 2008a, 2008b; Turbak, Snyder, & Sandberg, 1983 and references therein); chemical treatments, e.g., acid hydrolysis (for example, Araki, Wada, Kuga, & Okano, 2000; Elazzouzi-Hafraoui et al., 2007; Liu, Liu, Yao, & Wu, 2010); biological treatments, e.g., enzyme-assisted hydrolysis (see Hayashi,

* Corresponding author at: Material Science and Engineering College, Northeast Forestry University, No. 26 Hexing Road, Xiangfang District, Harbin 150040, China. Tel.: +86 451 8219 1756; fax: +86 451 8219 0134.
E-mail address: yuhaipeng20000@yahoo.com.cn (H. Yu).

0144-8617/$ – see front matter © 2010 Elsevier Ltd. All rights reserved.
doi:10.1016/j.carbpol.2010.10.040

Kondo, & Ishihara, 2005; Henriksson, Henriksson, Berglund, & Lindström, 2007; Pääkkö et al., 2007 and references therein); TEMPO-mediated oxidation on the surface of microfibrils and a subsequent mild mechanical treatment (see Iwamoto et al., 2010; Saito et al., 2009; Saito, Kimura, Nishiyama, & Isogai, 2007; Saito, Nishiyama, Putaux, Vignon, & Isogai, 2006 and references therein); synthetic and electrospinning methods (for example, Frenot, Henriksson, & Walkenström, 2007; Kim, Kim, Kang, Marquez, & Joo, 2006; Ma, Kotaki, & Ramakrishna, 2005); as well as a combination of two or several of the aforementioned methods. All these methods lead to different types of nanofibrillar materials, depending on the cellulose raw material and its pretreatment, and more importantly, depending on the disintegration process itself.

Recently, the ultrasonic technique as an emerging method to isolate cellulose nanofibers has been sufficiently described (Cheng, Wang, & Han, 2010; Cheng, Wang, Rials, & Lee, 2007; Cheng, Wang, & Rials, 2009; Wang & Cheng, 2009; Zhao, Feng, & Gao, 2007). Ultrasound energy is transferred to cellulose chains through a process called cavitation, which refers to the formation, growth, and violent collapse of cavities in water. The energy provided by cavitation in this so-called sonochemistry is approximately 10–100 kJ/mol, which is within the hydrogen bond energy scale (Tischer, Sierakowski, Westfahl, & Tischer, 2010). Thus, the ultrasonic impact can gradually disintegrate the micron-sized cellulose fibers into nanofibers. However, because of the complicated multilayered structure of plant fibers and the interfibrillar hydrogen bonds (Manley, 1964; Somerville et al., 2004), the fibers obtained by these methods are aggregated nanofibers with a wide distribution in width (Cheng et al., 2009).

Since cellulose nanofibers are embedded in matrix substances such as hemicellulose and lignin, a number of researchers have been removing the matrix substances using chemical methods before the fibrillation process and keeping the material in the water-swollen state. As a result, cellulose nanofibers with a uniform width can be obtained (Abe et al., 2007; Abe & Yano, 2009, 2010). Although chemical pretreatments have been successfully used in isolating nanofibers from cellulose or chitin (Fan, Saito, & Isogai, 2008; Ifuku et al., 2009) through the integration of grinding or the homogenizing process, there has been insufficient research on ultrasonic treatment. This study aims to individualize cellulose nanofibers from wood using high-intensity ultrasonication combined with chemical pretreatments. The morphological and structural characteristics of isolated nanofibers were analyzed through SEM and TEM, respectively. FTIR spectroscopy, XRD, and TGA experiments were performed to characterize the changes in the as-prepared products during the processing procedures.

2. Materials and methods

2.1. Raw materials

Wood powder from poplar trees sieved through a 60 mesh was used as the source of native cellulose fibers. All samples were air-dried and stored at room temperature. The sections were dewaxed in a Soxhlet apparatus with a 2:1 (v/v) mixture of benzene/ethanol at 90 °C for 6 h. Benzene, ethanol, sodium chlorite, acetic acid, potassium hydroxide, and other chemicals were of laboratory grade and used without further purification.

2.2. Preparation of nanofibers

The individualization process consists of chemical pretreatment and high-intensity ultrasonication (Fig. 1). In the chemical pretreatment stage, the wood fibers were purified to prepare the cellulose fibers according to general methods (Abe & Yano, 2009). First, lignin was removed from the samples using acidified sodium chlorite solution at 75 °C for an hour; this process was repeated five times until the product became white. Next, the samples were treated in 3 wt% potassium hydroxide at 80 °C for 2 h, and then in 6 wt% potassium hydroxide at 80 °C for 2 h in order to leach hemicellulose, residual starch, and pectin. After a series of chemical treatments, the samples were filtered and rinsed with distilled water until the residues were neutralized. To avoid generating strong hydrogen bonding among nanofibers after matrix removal, the samples were kept in a water-swollen state during the whole chemical process.

After chemical pretreatment, the purified cellulose fibers were soaked in distilled water (concentration: ~0.5% in mass). About 120 ml of solution containing chemical-purified cellulose fibers was then placed in a common ultrasonic generator (JY98-IIID, Ningbo Scientz Biotechnology Co., Ltd., China) of 20–25 kHz in frequency equipped with a cylindrical titanium alloy probe tip of 1.5 cm in diameter. The subsequent ultrasonication was conducted 30 min to isolate the nanofibers. To investigate the effect of ultrasonic intensity on the nanofibrillation of the chemical-purified cellulose fibers, the output power of the ultrasonication was conducted at 400, 800, 1000, and 1200 W, respectively. The ultrasonic treatment was carried out in an ice/water bath, and the ice was maintained throughout the entire ultrasonication time.

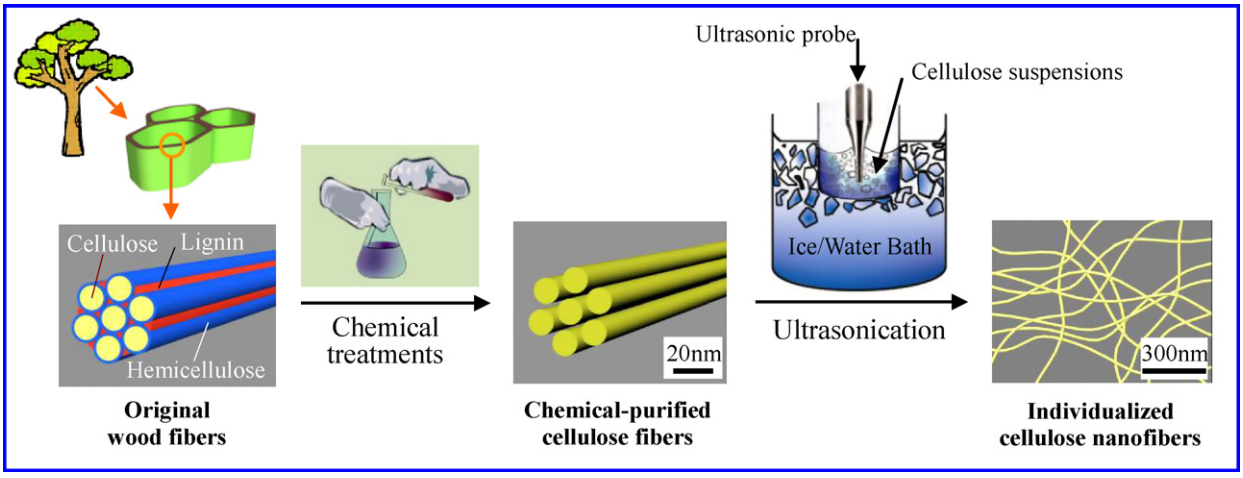

Fig. 1. Procedure for individualizing cellulose nanofibers.

2.3. Visual examination

The changes in dispersion of the cellulose suspensions after chemical pretreatment and ultrasonic treatment were observed through visual examination accomplished on cellulose–water slurries.

2.4. Scanning electron microscopy (FE-SEM)

The suspensions of the cellulose fibers before and after the ultrasonic process were subjected to freeze-drying after water was replaced with t-butyl alcohol. The obtained sheets were coated with gold using a vacuum sputter coater and then observed with FE-SEM (Sirion 200, FEI, Netherlands).

2.5. Transmission electron microscopy (TEM)

Drops of dilute cellulose nanofiber suspensions were deposited into glow-discharged carbon-coated TEM grids. The excess liquid was absorbed by a piece of filter paper. After the specimen has been completely dried, it was observed using a FEI Tecnai G2 electron microscope operated at 80 kV. The diameters of the cellulose nanofibers were calculated from TEM images using microscope image analysis system (TDY-V5.2, Beijing Tianhong Precision Instrument Technology Co., Ltd., China), which were used to illustrate size distributions.

2.6. Fourier transform infrared (FTIR) spectroscopy

The FTIR spectra were recorded on a Fourier transform infrared (FTIR) instrument (Magna 560, Nicolet, Thermo Electron Corp., USA) in the range of 400–4000 cm^{-1} with a resolution of 4 cm^{-1}. The dried samples were ground into powder by a fiber microtome and then blended with KBr before pressing the mixture into ultrathin pellets.

2.7. X-ray diffraction analysis

The X-ray diffraction (XRD) patterns were measured for raw wood fibers, chemical-purified cellulose fibers, and isolated nanofibers with an X-ray diffractometer (D/max 2200, Rigaku, Japan) using Ni-filtered Cu Kα radiation (λ = 1.5406 Å) at 40 kV and 30 mA. Scattered radiation was detected in the range of $2\theta = 10–30^\circ$ at a scan rate of 4°/min. The crystallinity index (C_I) was calculated from the heights of the 2 0 0 peak (I_{200}, $2\theta = 22.6^\circ$) and the intensity minimum between the 2 0 0 and 1 1 0 peaks (I_{am}, $2\theta = 18^\circ$) using the Segal method (Eq. (1)). I_{200} represents both crystalline and amorphous material, whereas I_{am} represents the amorphous material.

$$C_I(\%) = \left(1 - \frac{I_{am}}{I_{200}}\right) \times 100 \quad (1)$$

2.8. Thermal characterization

Thermogravimetric analysis was performed to compare the degradation characteristics of the raw wood fibers, chemical-purified cellulose fibers, and cellulose nanofibers obtained using ultrasonic treatment with different output powers. The thermal stability of each sample was determined using a thermogravimetric analyzer (Pyris 6, PerkinElmer, USA) with a heating rate of 10 °C/min in a nitrogen environment.

3. Results and discussion

3.1. Visual examination

The aqueous suspensions of the original wood fibers, chemical-purified cellulose fibers, and cellulose nanofibers after 30 min of ultrasonic treatment with an output power of 400, 800, 1000, and 1200 W, respectively, were placed motionlessly at least 30 min after they were prepared, and then the photos in Fig. 2 were taken. Raw wood fibers and chemical-purified cellulose fibers were precipitated at the bottom of the glass bottle; brown wood fibers became white after chemical purification, indicating that a significant amount of lignin was removed. After ultrasonic treatment, a substantial increase in the dispersion of the nanofiber suspensions was observed when the ultrasonic output power increased from 400 to 1200 W. Although the cellulose nanofibers were not homogenously dispersed in water at 400 W, there was a noticeable improvement when the output power increased to 800 W. After an output power of 1000 or 1200 W was conducted, a more colloidal structure was obtained. Then the cellulose nanofibers were sufficiently dispersed and converted to highly viscous suspensions. This finding indicated that there was an improvement in the degree of nanofibrillation of the cellulose fibers, and more surface area on the nanofibers was exposed as the ultrasonic output power increased.

3.2. Morphology of the chemical-purified cellulose fibers and cellulose nanofibers

Fig. 3 shows the FE-SEM images of the chemical-purified cellulose fibers. After chemical pretreatment, the cellulose fibers were separated into individual micro-sized fibers. In fact, these micro-sized fibers were reportedly composed of strong hydrogen bonding nanofibers, and individualized nanofiber bundles with a width of 10–30 nm can be seen on the surface of the micro-sized cellulose fiber (Fig. 3c). However, the samples still maintained the initial cell shape (Fig. 3b). After ultrasonic treatment, individual nanofibers can be obtained.

Fig. 4 compares the TEM images of the isolated nanofibers obtained after a 30 min high-intensity ultrasonication treatment at various output powers. The diameter distributions of the nanofibers were analyzed; the result is also plotted in Fig. 4.

When the output power of ultrasonication was conducted at 400 W, large aggregates consisting of wire-like cellulose fibers with nanoscale widths were frequently observed; a number of branches of smaller bundles or partly individualized nanofibers were attached to the large aggregates as well. Although nearly 62% of the nanofibers were shorter than 20 nm, the diameter distribution of the cellulose fibers exhibited a wide array of sizes, ranging from several nanometers to several hundred nanometers. The number of individualized cellulose nanofibers increased for

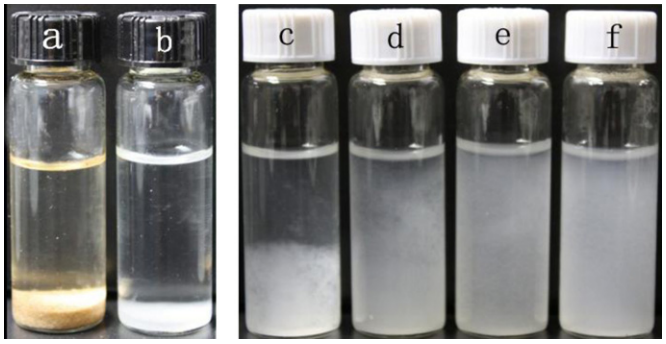

Fig. 2. Dispersion states of the (a) original wood fibers, (b) chemical-purified cellulose fibers, (c) cellulose nanofibers with ultrasonic output power of 400 W, (d) 800 W, (e) 1000 W and (f) 1200 W.

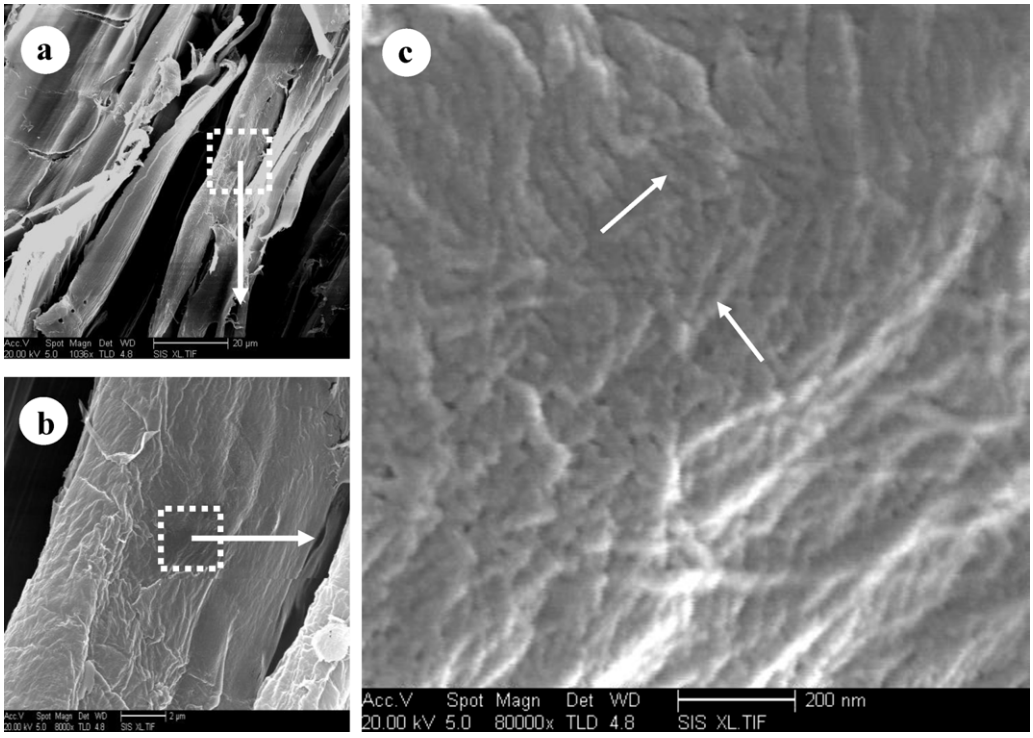

Fig. 3. FE-SEM micrographs of the (a) chemical-purified cellulose fibers (1036×), (b) a chemical-purified cellulose fiber (8000×) and (c) the surface of the chemical-purified cellulose fiber (80,000×).

the ultrasonic output power conducted at 800 W, and more than 75% of the nanofibers had a diameter range of 5–20 nm. Although bundles of the nanofibers still existed to a certain extent in the suspension, small gaps among the unindividualized nanofibers can be observed in the nanofiber aggregates (insert image of Fig. 4b). This indicates that the hydrogen bonding between the nanofibers was lower after ultrasonic treatment at 800 W. Sequentially, chemical-purified cellulose fibers were subjected to 1000 W and 1200 W ultrasonic treatments, and cellulose nanofibers with a uniform width ranging from 5 to 20 nm and a web-like network structure were obtained. The average diameter of the obtained nanofibers was found to be 13.0 and 12.8 nm, respectively. The TEM observation also revealed that the length of most obtained cellulose nanofibers was a few microns. When cellulose nanofibers prepared with 1000 and 1200 W ultrasonic treatment were observed using FE-SEM (Fig. 5) after gold sputtering, fibers in the nano-order scale and entangled structure were also observed, which satisfactorily agreed with TEM measurements. It is probable that the nanofibers were covered with relatively thick gold layers by the sputtering process, which is necessary to observe such nanoscale cellulose fibers by FE-SEM. It is thus illustrated that the degree of nanofibrillation depends on the output power of the ultrasonic treatment, i.e., the obtained nanofibers become more uniform and slender with increased intensity. The result indicated that ultrasonic treatments with an output power equal or greater than 1000 W can efficiently individualize cellulose nanofibers and disperse them in an aqueous suspension. This approach to individualize nanofibers from wood chemical-purified cellulose fibers may be explained by the effect of acoustic cavitation of high frequency (20–25 kHz) ultrasound in the formation, expansion, and implosion of microbubbles in aqueous solution. The violent collapse induces microjets and shock waves on the surfaces of the chemical-purified cellulose fibers, causing erosion of the surface of the fibers to split along the axial direction. The sonification impact can break the relatively weak interfaces among the nanofibers, which are bonded to each other mainly by hydrogen bonds. Thus the ultrasonic treatment can gradually disintegrate the micron sized cellulose fibers into nanofibers (Tischer et al., 2010; Wang & Cheng, 2009; Zhao et al., 2007).

3.3. Chemical structure analysis with FTIR spectroscopy

FTIR spectroscopy is an appropriate technique in establishing the variations introduced by different treatments on the chemical structure of the isolated samples. Fig. 6 compares the FTIR spectra of raw wood fibers, chemical-purified cellulose fibers, and cellulose nanofibers after ultrasonic treatments. The dominant peaks of OH-stretching and CH-stretching at approximately 3400 cm^{-1} and 2800 cm^{-1} were observed in the entire spectra. After $NaClO_2$ and KOH treatment, the prominent peak of the raw wood fibers at 1737 cm^{-1}, which is attributed either to the acetyl and uronic ester groups of the hemicellulose or to the ester linkage of the carboxylic groups of the ferulic and p-coumeric acids of lignin and/or hemicellulose (Sain & Panthapulakkal, 2006; Sun, Tomkinson, Wang, & Xiao, 2000), disappeared completely. This indicates that most of the hemicellulose and lignin were removed from the wood fibers during the step-wise chemical treatment. The 1507 and 1460 cm^{-1} peaks in the wood fibers represent aromatic ring vibration and C–H deformation vibration of lignin, respectively (Sain & Panthapulakkal, 2006; Sun et al., 2000). The intensity of these peaks disappeared in the chemical-purified cellulose fibers, which is attributed to the removal of lignin. The 1640 cm^{-1} peak in the raw wood fibers is associated with the H–O–H stretching vibration of absorbed water in carbohydrates. It was still observed in the chemical-purified cellulose fibers, although the intensity slightly declined. This indicates that a small amount of hemicellulose still exists in the purified cellulose fibers, which plays a positive role in the facilitation of nanofibrillation (Herrick et al., 1983; Turbak et al., 1983). Other peaks, i.e., 1061 and 897 cm^{-1} peaks, are associated with the C–O stretching and C_1–H deformation vibrations of cellulose (Alemdar & Sain, 2008), which appeared in all spec-

tra. Interestingly, no difference was found between the spectrum of cellulose nanofibers obtained under different ultrasonic output powers and chemical-purified cellulose fibers. This result suggests that the molecular structures of cellulose were unchanged in the case of ultrasonic treatment.

3.4. Crystal structure analysis by X-ray diffraction

Cellulose crystallinity in individualized nanofibers as the key factor determining their mechanical and thermal properties is of interest. XRD studies on treated and untreated cellulose fibers were

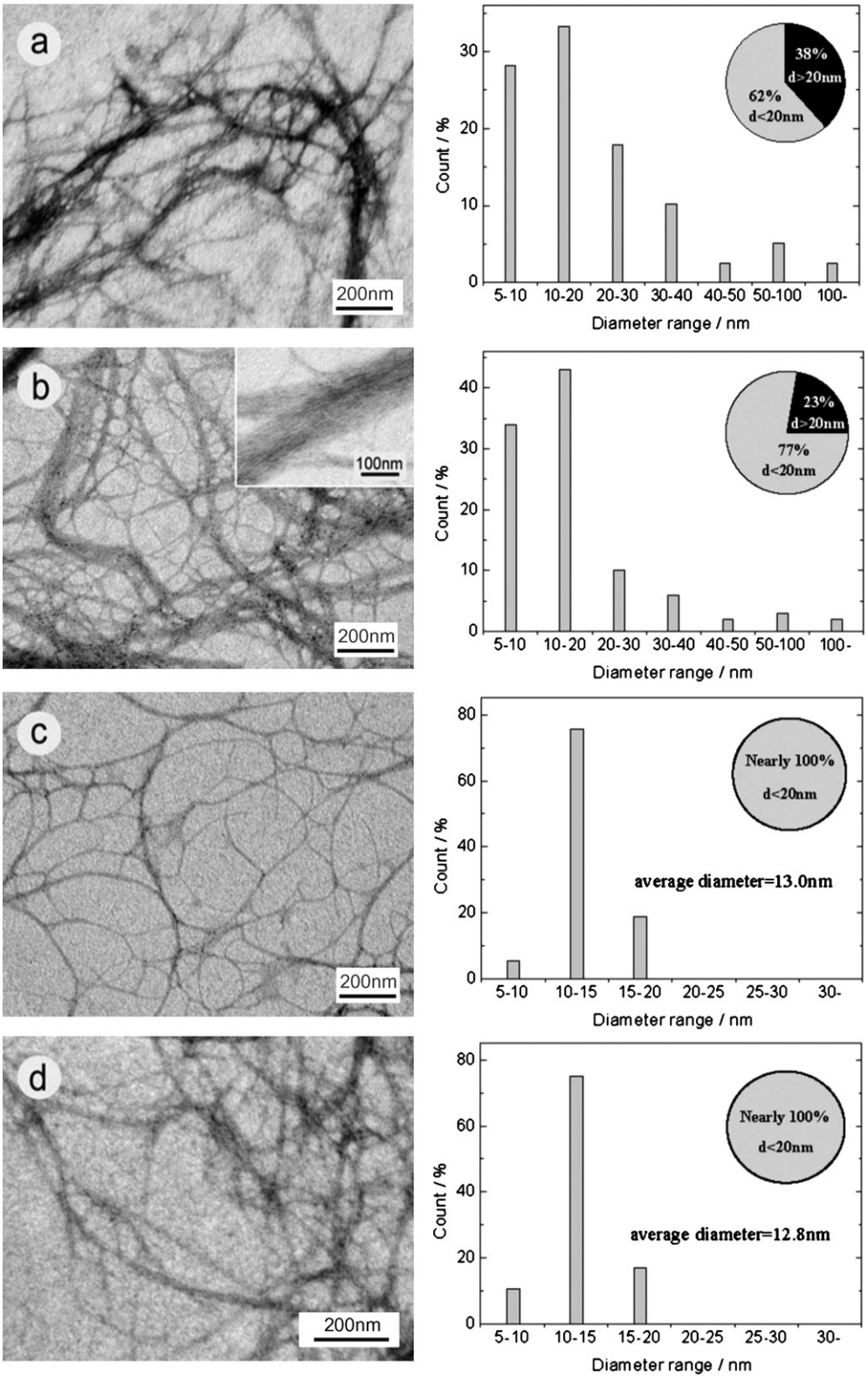

Fig. 4. TEM micrographs and diameter distribution of the cellulose nanofibers after ultrasonic treatment with various output power. (a) 400 W, (b) 800 W, (c) 1000 W and (d) 1200 W.

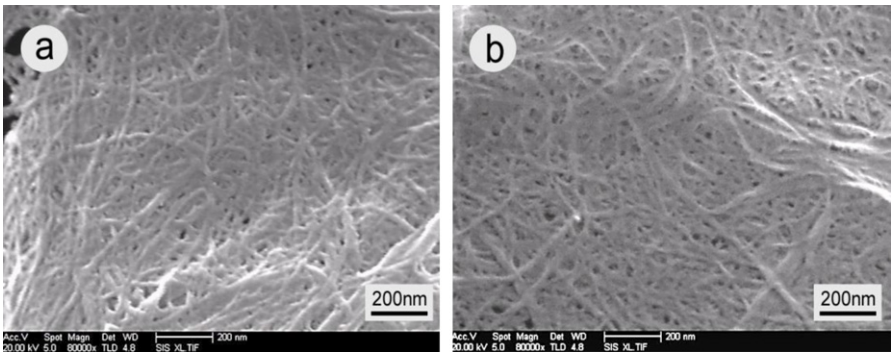

Fig. 5. FE-SEM micrographs of the wood cellulose nanofibers after ultrasonic treatment with output power of (a) 1000 W and (b) 1200 W.

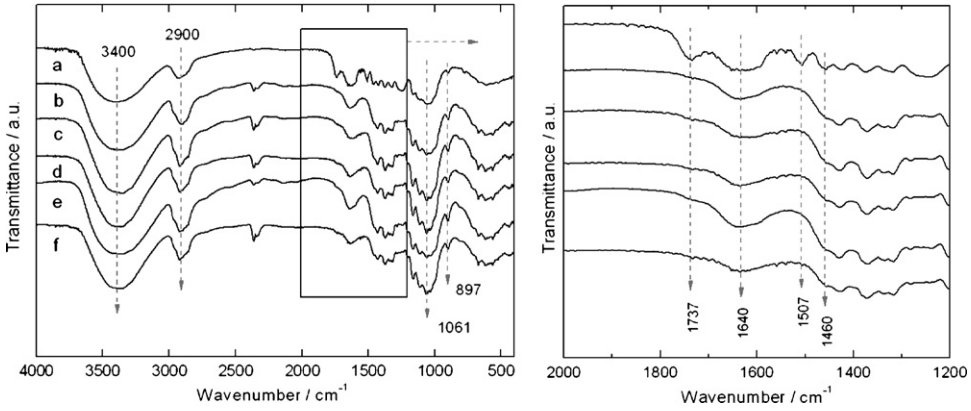

Fig. 6. FTIR spectra of the (a) original wood fibers, (b) chemical-purified cellulose fibers, (c) cellulose nanofibers with ultrasonic output power of 400 W, (d) 800 W, (e) 1000 W and (f) 1200 W.

conducted to investigate the crystalline behavior of the fibers. The XRD graph (Fig. 7) evidently shows that all diffractograms exhibited sharp peaks around $2\theta = 16^\circ$ and 22.6°, which were believed to represent typical cellulose I form. This indicates that the crystal structure of cellulose was not changed during the chemical and ultrasonic treatment. The crystallinity of each sample is also calculated and listed in Fig. 7. A significant increase in crystallinity from 52.74% for the original wood fibers to 69.34% for the chemical-purified cellulose fibers was observed. The increase in crystallinity was undoubtedly due to the removal of hemicellulose and lignin, which exist in amorphous regions. This leads to the realignment of cellulose molecules. The increase in crystallinity after chemical treatments has been reported by several authors (Alemdar & Sain, 2008; Li et al., 2009). After ultrasonic treatment, no significant differences appeared between isolated nanofibers and chemical-purified cellulose fibers; the crystallinity of each nanofiber was around 69%, implying that the ultrasonic treatment had little effect on the crystal regions of the cellulose nanofibers. These results were also supported by the FTIR analyses. High crystalline nanofibers can be more effective in achieving higher reinforcement for composite materials.

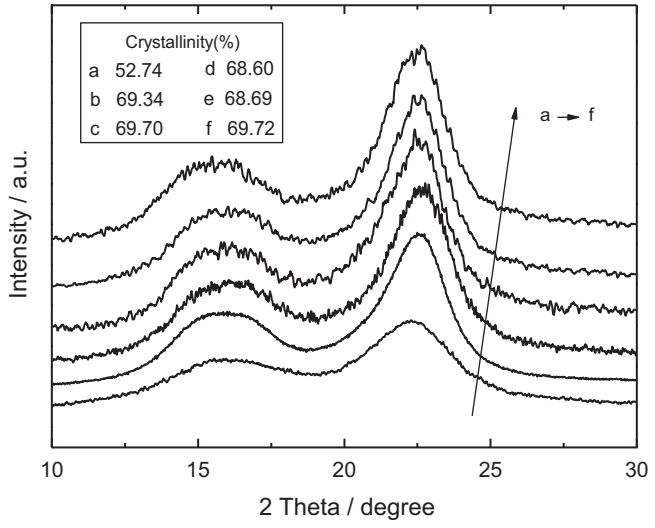

Fig. 7. X-ray diffraction patterns of the (a) original wood fibers, (b) chemical-purified cellulose fibers, (c) cellulose nanofibers with ultrasonic output power of 400 W, (d) 800 W, (e) 1000 W and (f) 1200 W.

3.5. Thermostability analysis

An examination of the thermal properties of cellulose fibers is important in gauging their applicability in bio-composite processing, wherein the processing temperature for thermoplastic polymers increases above 200 °C. Fig. 8 shows the TG curves of the original wood fibers, chemical-purified cellulose fibers, and cellulose nanofibers obtained after ultrasonic treatments. In all cases, a small weight loss was found in the range of 25–150 °C due to the evaporation of the humidity of the materials or the low molecular weight compounds remaining from the isolation procedures. Due to the low decomposition temperature of hemicellulose, lignin, and pectin (Morán et al., 2008), the curve of the original wood fibers shows an earlier weight loss that started at around 210 °C, which reached the dominant peak at 350 °C on the DTG curve, accounting for the pyrolysis of cellulose. On the other hand, the chemical-purified cellulose fibers showed a higher decomposition temperature at 335 °C. The higher temperature of thermal decom-

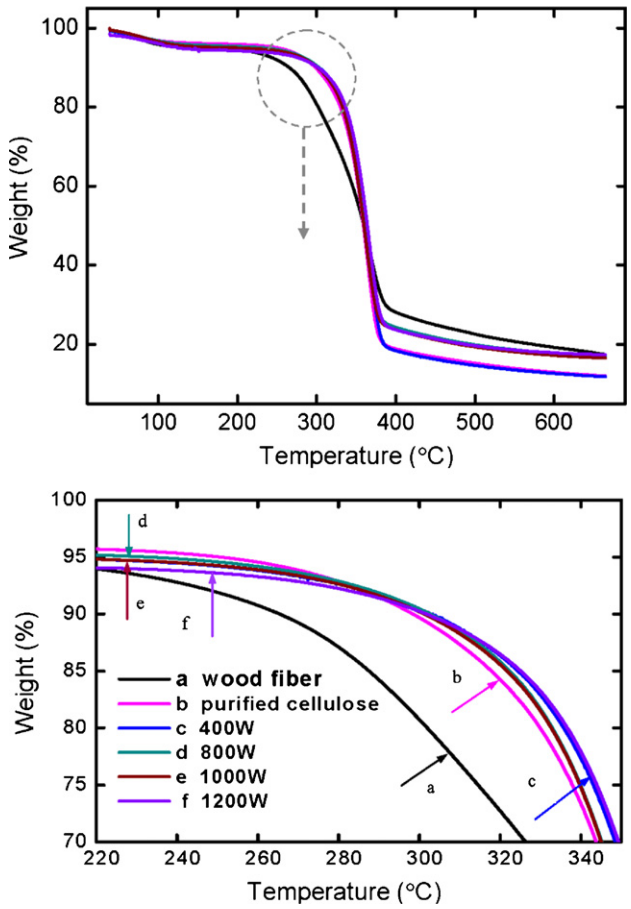

Fig. 8. TG curves of the (a) original wood fibers, (b) chemical-purified cellulose fibers, (c) cellulose nanofibers with ultrasonic output power of 400 W, (d) 800 W, (e) 1000 W and (f) 1200 W.

position of the purified cellulose fibers is related to the partial removal of hemicellulose and lignin from the fibers, as well as the higher crystallinity of cellulose (Alemdar & Sain, 2008). The cellulose nanofibers obtained after ultrasonic treatments exhibited a degradation behavior that is highly similar to that of the purified cellulose fibers. The decomposition temperature of all cellulose nanofibers under different ultrasonic output powers starting at approximately 335 °C, implied that ultrasonic treatment had little effect on the thermal decomposition of the cellulose nanofibers. This result is also consistent with the findings obtained from the XRD and FTIR analyses, indicating that the ultrasonic process did not influence cellulose chemical composition, crystal structure, and thermostability. Apparently, only structural changes occurred.

4. Conclusion

Cellulose nanofibers were individualized from poplar wood using chemical pretreatment and high-intensity ultrasonication. When the output power of ultrasonic treatment used for the chemical-purified cellulose fibers was greater than 1000 W, cellulose nanofibers that are 5–20 nm in width and several microns in length were obtained. FTIR measurements of the fibers revealed that there was partial removal of hemicellulose and lignin because of the successful chemical treatments applied. The relative crystallinity of the cellulose nanofibers reached approximately 69%. The nanofibers also exhibited enhanced thermal properties, and the thermal degradation temperature increased to approximately 335 °C.

Acknowledgement

This work was financially supported by the Fundamental Research Funds for the Central Universities (DL09EB01-3). This work was also supported by Program for the Top Young Talents of Northeast Forestry University, and the Programme of Introducing Talents of Discipline to Universities of China (B08016).

References

Abe, K., Iwamoto, S., & Yano, H. (2007). Obtaining cellulose nanofibers with a uniform width of 15 nm from wood. *Biomacromolecules*, *8*(10), 3276–3278.
Abe, K., Nakatsubo, F., & Yano, H. (2009). High-strength nanocomposite based on fibrillated chemi-thermomechanical pulp. *Composites Science and Technology*, *69*(14), 2434–2437.
Abe, K., & Yano, H. (2009). Comparison of the characteristics of cellulose microfibril aggregates of wood, rice straw and potato tuber. *Cellulose*, *16*(6), 1017–1023.
Abe, K., & Yano, H. (2010). Comparison of the characteristics of cellulose microfibril aggregates isolated from fiber and parenchyma cells of Moso bamboo (*Phyllostachys pubescens*). *Cellulose*, *17*(2), 271–277.
Alemdar, A., & Sain, M. (2008). Isolation and characterization of nanofibers from agricultural residues – Wheat straw and soy hulls. *Bioresource Technology*, *99*(6), 1664–1671.
Araki, J., Wada, M., Kuga, S., & Okano, T. (2000). Birefringent glassy phase of a cellulose microcrystal suspension. *Langmuir*, *16*(6), 2413–2415.
Azizi Samir, M. A. S., Alloin, F., & Dufresne, A. (2005). Review of recent research into cellulosic whiskers, their properties and their application in nanocomposite field. *Biomacromolecules*, *6*(2), 612–626.
Chakraborty, A., Sain, M., & Kortschot, M. (2005). Cellulose microfibrils: A novel method of preparation using high shear refining and cryocrushing. *Holzforschung*, *59*(1), 102–107.
Chakraborty, A., Sain, M., & Kortschot, M. (2006). Reinforcing potential of wood pulp-derived microfibres in a PVA matrix. *Holzforschung*, *60*(1), 53–58.
Chen, Y., Liu, C., Chang, P. R., Cao, X., & Anderson, D. P. (2009). Bionanocomposites based on pea starch and cellulose nanowhiskers hydrolyzed from pea hull fibre: Effect of hydrolysis time. *Carbohydrate Polymers*, *76*(4), 607–615.
Cheng, Q., Wang, S., & Han, Q. (2010). Novel process for isolating fibrils from cellulose fibers by high-intensity ultrasonication. II. Fibril characterization. *Journal of Applied Polymer Science*, *115*(5), 2756–2762.
Cheng, Q., Wang, S., Rials, T., & Lee, S. (2007). Physical and mechanical properties of polyvinyl alcohol and polypropylene composite materials reinforced with fibril aggregates isolated from regenerated cellulose fibers. *Cellulose*, *14*(6), 593–602.
Cheng, Q., Wang, S., & Rials, T. G. (2009). Poly(vinyl alcohol) nanocomposites reinforced with cellulose fibrils isolated by high intensity ultrasonication. *Composites Part A: Applied Science and Manufacturing*, *40*(2), 218–224.
Cherian, B. M., Leão, A. L., de Souza, S. F., Thomas, S., Pothan, L. A., & Kottaisamy, M. (2010). Isolation of nanocellulose from pineapple leaf fibres by steam explosion. *Carbohydrate Polymers*, *81*(3), 720–725.
de Morais Teixeira, E., Corrêa, A., Manzoli, A., de Lima Leite, F., de Oliveira, C., & Mattoso, L. (2010). Cellulose nanofibers from white and naturally colored cotton fibers. *Cellulose*, *17*(3), 595–606.
Dinand, E., Chanzy, H., & Vignon, R. M. (1999). Suspensions of cellulose microfibrils from sugar beet pulp. *Food Hydrocolloids*, *13*(3), 275–283.
Dufresne, A., Cavaillé, J. Y., & Vignon, M. R. (1997). Mechanical behavior of sheets prepared from sugar beet cellulose microfibrils. *Journal of Applied Polymer Science*, *64*(6), 1185–1194.
Dufresne, A., Dupeyre, D., & Vignon, M. R. (2000). Cellulose microfibrils from potato tuber cells: Processing and characterization of starch-cellulose microfibril composites. *Journal of Applied Polymer Science*, *76*(14), 2080–2092.
Eichhorn, S., Dufresne, A., Aranguren, M., Marcovich, N., Capadona, J., Rowan, S., et al. (2010). Review: Current international research into cellulose nanofibres and nanocomposites. *Journal of Materials Science*, *45*(1), 1–33.
Elazzouzi-Hafraoui, S., Nishiyama, Y., Putaux, J.-L., Heux, L., Dubreuil, F., & Rochas, C. (2007). The shape and size distribution of crystalline nanoparticles prepared by acid hydrolysis of native cellulose. *Biomacromolecules*, *9*(1), 57–65.
Fan, Y., Saito, T., & Isogai, A. (2008). Preparation of chitin nanofibers from squid pen β-chitin by simple mechanical treatment under acid conditions. *Biomacromolecules*, *9*(7), 1919–1923.
Frenot, A., Henriksson, M. W., & Walkenström, P. (2007). Electrospinning of cellulose-based nanofibers. *Journal of Applied Polymer Science*, *103*(3), 1473–1482.
Fukuzumi, H., Saito, T., Iwata, T., Kumamoto, Y., & Isogai, A. (2009). Transparent and high gas barrier films of cellulose nanofibers prepared by TEMPO-mediated oxidation. *Biomacromolecules*, *10*(1), 162–165.
Habibi, Y., Heux, L., Mahrouz, M., & Vignon, M. R. (2008). Morphological and structural study of seed pericarp of *Opuntia ficus-indica* prickly pear fruits. *Carbohydrate Polymers*, *72*(1), 102–112.
Hayashi, N., Kondo, T., & Ishihara, M. (2005). Enzymatically produced nano-ordered short elements containing cellulose I_β crystalline domains. *Carbohydrate Polymers*, *61*(2), 191–197.
Henriksson, M., Henriksson, G., Berglund, L. A., & Lindström, T. (2007). An environmentally friendly method for enzyme-assisted preparation of microfibrillated cellulose (MFC) nanofibers. *European Polymer Journal*, *43*, 3434–3441.

Herrick, F. W., Casebier, R. L., & Hamilton, J. K. (1983). Microfibrillated cellulose: Morphology and accessibility. *Journal of Applied Polymer Science: Applied Polymer Symposium*, *37*, 797–813.

Ifuku, S., Nogi, M., Abe, K., Yoshioka, M., Morimoto, M., Saimoto, H., et al. (2009). Preparation of chitin nanofibers with a uniform width as α-chitin from crab shells. *Biomacromolecules*, *10*(6), 1584–1588.

Iwamoto, S., Kai, W., Isogai, T., Saito, T., Isogai, A., & Iwata, T. (2010). Comparison study of TEMPO-analogous compounds on oxidation efficiency of wood cellulose for preparation of cellulose nanofibrils. *Polymer Degradation and Stability*, *95*(8), 1394–1398.

Iwamoto, S., Nakagaito, A. N., & Yano, H. (2007). Nano-fibrillation of pulp fibers for the processing of transparent nanocomposites. *Applied Physics A: Materials Science & Processing*, *89*(2), 461–466.

Kim, C. W., Kim, D. S., Kang, S. Y., Marquez, M., & Joo, Y. L. (2006). Structural studies of electrospun cellulose nanofibers. *Polymer*, *47*(14), 5097–5107.

Li, R., Fei, J., Cai, Y., Li, Y., Feng, J., & Yao, J. (2009). Cellulose whiskers extracted from mulberry: A novel biomass production. *Carbohydrate Polymers*, *76*(1), 94–99.

Liu, H., Liu, D., Yao, F., & Wu, Q. (2010). Fabrication and properties of transparent polymethylmethacrylate/cellulose nanocrystals composites. *Bioresource Technology*, *101*(14), 5685–5692.

Ma, Z., Kotaki, M., & Ramakrishna, S. (2005). Electrospun cellulose nanofiber as affinity membrane. *Journal of Membrane Science*, *265*(1–2), 115–123.

Malainine, M. E., Dufresne, A., Dupeyre, D., Mahrouz, M., Vuong, R., & Vignon, M. R. (2003). Structure and morphology of cladodes and spines of *Opuntia ficus-indica*. Cellulose extraction and characterisation. *Carbohydrate Polymers*, *51*(1), 77–83.

Manley, R. S. J. (1964). Fine structure of native cellulose microfibrils. *Nature*, *204*(4964), 1155–1157.

Morán, J., Alvarez, V., Cyras, V., & Vázquez, A. (2008). Extraction of cellulose and preparation of nanocellulose from sisal fibers. *Cellulose*, *15*(1), 149–159.

Nakagaito, A., & Yano, H. (2008a). The effect of fiber content on the mechanical and thermal expansion properties of biocomposites based on microfibrillated cellulose. *Cellulose*, *15*(4), 555–559.

Nakagaito, A., & Yano, H. (2008b). Toughness enhancement of cellulose nanocomposites by alkali treatment of the reinforcing cellulose nanofibers. *Cellulose*, *15*(2), 323–331.

Nakagaito, A. N., & Yano, H. (2004). The effect of morphological changes from pulp fiber towards nano-scale fibrillated cellulose on the mechanical properties of high-strength plant fiber based composites. *Applied Physics A: Materials Science & Processing*, *78*(4), 547–552.

Nakagaito, A. N., & Yano, H. (2005). Novel high-strength biocomposites based on microfibrillated cellulose having nano-order-unit web-like network structure. *Applied Physics A: Materials Science & Processing*, *80*(1), 155–159.

Nishino, T., Matsuda, I., & Hirao, K. (2004). All-cellulose composite. *Macromolecules*, *37*(20), 7683–7687.

Nogi, M., Iwamoto, S., Nakagaito, A. N., & Yano, H. (2009). Optically transparent nanofiber paper. *Advanced Materials*, *21*(16), 1595–1598.

Orts, W. J., Shey, J., Imam, S. H., Glenn, G. M., Guttman, M. E., & Revol, J.-F. (2005). Application of cellulose microfibrils in polymer nanocomposites. *Journal of Polymers and the Environment*, *13*(4), 301–306.

Pääkkö, M., Ankerfors, M., Kosonen, H., Nykänen, A., Ahola, S., Österberg, M., et al. (2007). Enzymatic hydrolysis combined with mechanical shearing and high-pressure homogenization for nanoscale cellulose fibrils and strong gels. *Biomacromolecules*, *8*(6), 1934–1941.

Rondeau-Mouro, C., Bouchet, B., Pontoire, B., Robert, P., Mazoyer, J., & Buléon, A. (2003). Structural features and potential texturising properties of lemon and maize cellulose microfibrils. *Carbohydrate Polymers*, *53*(3), 241–252.

Rosa, M. F., Medeiros, E. S., Malmonge, J. A., Gregorski, K. S., Wood, D. F., Mattoso, L. H. C., et al. (2010). Cellulose nanowhiskers from coconut husk fibers: Effect of preparation conditions on their thermal and morphological behavior. *Carbohydrate Polymers*, *81*(1), 83–92.

Sain, M., & Panthapulakkal, S. (2006). Bioprocess preparation of wheat straw fibers and their characterization. *Industrial Crops and Products*, *23*(1), 1–8.

Saito, T., Hirota, M., Tamura, N., Kimura, S., Fukuzumi, H., Heux, L., et al. (2009). Individualization of nano-sized plant cellulose fibrils by direct surface carboxylation using TEMPO catalyst under neutral conditions. *Biomacromolecules*, *10*(7), 1992–1996.

Saito, T., Kimura, S., Nishiyama, Y., & Isogai, A. (2007). Cellulose nanofibers prepared by TEMPO-mediated oxidation of native cellulose. *Biomacromolecules*, *8*(8), 2485–2491.

Saito, T., Nishiyama, Y., Putaux, J. L., Vignon, M., & Isogai, A. (2006). Homogeneous suspensions of individualized microfibrils from TEMPO-catalyzed oxidation of native cellulose. *Biomacromolecules*, *7*(6), 1687–1691.

Siró, I., & Plackett, D. (2010). Microfibrillated cellulose and new nanocomposite materials: A review. *Cellulose*, *17*, 459–494.

Somerville, C., Bauer, S., Brininstool, G., Facette, M., Hamann, T., Milne, J., et al. (2004). Toward a systems approach to understanding plant cell walls. *Science*, *306*(5705), 2206–2211.

Sun, R. C., Tomkinson, J., Wang, Y. X., & Xiao, B. (2000). Physico-chemical and structural characterization of hemicelluloses from wheat straw by alkaline peroxide extraction. *Polymer*, *41*(7), 2647–2656.

Syverud, K., & Stenius, P. (2009). Strength and barrier properties of MFC films. *Cellulose*, *16*(1), 75–85.

Tischer, P. C. S. F., Sierakowski, M. R., Westfahl, H., & Tischer, C. A. (2010). Nanostructural reorganization of bacterial cellulose by ultrasonic treatment. *Biomacromolecules*, *11*(5), 1217–1224.

Turbak, A. F., Snyder, F. W., & Sandberg, K. R. (1983). Microfibrillated cellulose, a new cellulose product: Properties, uses, and commercial potential. *Journal of Applied Polymer Science: Applied Polymer Symposium*, *37*, 815–827.

Wang, B., & Sain, M. (2007). Isolation of nanofibers from soybean source and their reinforcing capability on synthetic polymers. *Composites Science and Technology*, *67*(11–12), 2521–2527.

Wang, B., Sain, M., & Oksman, K. (2007). Study of structural morphology of hemp fiber from the micro to the nanoscale. *Applied Composite Materials*, *14*(2), 89–103.

Wang, S., & Cheng, Q. (2009). A novel process to isolate fibrils from cellulose fibers by high-intensity ultrasonication. Part 1: Process optimization. *Journal of Applied Polymer Science*, *113*(2), 1270–1275.

Yano, H., Sugiyama, J., Nakagaito, A. N., Nogi, M., Matsuura, T., Hikita, M., et al. (2005). Optically transparent composites reinforced with networks of bacterial nanofibers. *Advanced Materials*, *17*(2), 153–155.

Zhao, H. P., Feng, X. Q., & Gao, H. (2007). Ultrasonic technique for extracting nanofibers from nature materials. *Applied Physics Letters*, *90*, 073112.

Zuluaga, R., Putaux, J. L., Cruz, J., Vélez, J., Mondragon, I., & Gañán, P. (2009). Cellulose microfibrils from banana rachis: Effect of alkaline treatments on structural and morphological features. *Carbohydrate Polymers*, *76*(1), 51–59.